



ANALYSIS OF THE VOID VOLUME FRACTION FOR S235JR STEEL AT FAILURE FOR LOW INITIAL STRESS TRIAXIALITY

P. G. KOSSAKOWSKI¹

Abstract. This paper deals with problems of failure mechanisms of S235JR structural steel. One of the fundamental parameters of the Gurson-Tvergaard-Needleman damage mechanics-based material model is considered in order to describe the behaviour of the material at the plastic range. The analysis was performed on the void volume fraction f_F determined at failure of S235JR steel. The case of low initial stress triaxiality $\eta = 1/3$ was taken into consideration. Different from the most popular methods such as curve-fitting, the experimental method based on the digital image analysis of the fracture surface of S235JR steel is proposed in order to determine the critical parameter f_F .

Keywords: void volume fraction, failure, S235JR steel, Gurson-Tvergaard-Needleman material model, low stress triaxiality.

1. INTRODUCTION

Although one of the first studies in the field of damage mechanics has been already established in the mid-twentieth century by Kachanov [1], and, later, by other authors [2-14], the problem of the exact determination of the failure processes of a variety of materials remains still unsolved. This also applies to structural steel, whose categories used in construction are subjected to the mechanisms of failure known as ductile fractures. They occur at the microstructural level, and the individual steps of this process

¹ DSc., PhD., Eng., Kielce University of Technology, Faculty of Civil Engineering and Architecture, Al. Tysiąclecia Państwa Polskiego 7, 25-314 Kielce, Poland, e-mail: kossak@tu.kielce.pl

are shown schematically in Fig. 1. The failure is triggered by microdefects, denoted as voids, which form both in the material matrix as well as foreign-phase precipitates and inclusions (nucleation phase). During the deformation process, the voids are growing, which leads to their coalescence. This is the main factor creating conditions to form a crack, which propagates up to final decohesion of the material. As the effects of the damage processes are taking place starting from the time when microdefects begin to grow, the nominal stresses become increasingly smaller until the material fails.

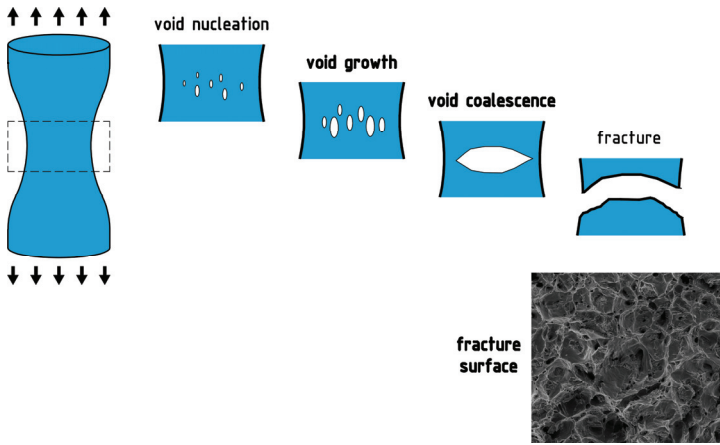


Fig. 1. Mechanism of ductile fracture (based on [15, 16])

Changes of the stress state observed during ductile fracture were attempted in order to describe usage of different material models. One of the widely developed was the model presented by Gurson in 1977 [2]. By defining the void volume fraction as a damage parameter, he took into consideration the influence of the number of microdefects on the material strength. In subsequent years, Gurson's concept was extensively developed and modified [17, 18], while the last important change was the introduction by Nahshon and Huthinson of the effect of a shear into the void evolution law [19]. After these developments, the modified Gurson function, denoted the most often as the Gurson-Tveergard-Needleman (GTN) yield-potential function, is presented in the form:

$$\Phi = \left(\frac{\sigma_e}{\sigma_0} \right)^2 + 2q_1 f^* \cosh \left(-q_2 \frac{3\sigma_m}{2\sigma_0} \right) - (1 + q_3 f^{*2}) = 0 \quad (1)$$

where: σ_e – effective stress defined according to the Huber-Mises-Hencky strength hypothesis $\sigma_e = \frac{1}{\sqrt{2}} \sqrt{(\sigma_1 - \sigma_2)^2 + (\sigma_2 - \sigma_3)^2 + (\sigma_1 - \sigma_3)^2}$ (with $\sigma_1, \sigma_2, \sigma_3$ being the principal stresses), σ_0 – flow stress of the matrix material (yield stress), σ_m – hydrostatic stress, f^* – modified void volume fraction and q_i – Tvergaard coefficients.

As can be seen in eq. (1), the Gurson plastic potential function is a much more complicated form of the classic Huber criterion based on continuum solid mechanics due to the introduction of the effect of material microdefects on the stress state. In order to describe the GTN material it is necessary to define several parameters. There are multiple studies concerning GTN parameters for many metals, but it is still necessary to analyse and determine them for structural steel used in construction, eg. [20-24], due to a lack of data for many basic grades.

One of the significant parameters which determines the process of material failure in the GTN material model is void volume fraction f_F , recognized at the time of material decohesion. For this reason, it is a criterion parameter which determines the total collapse of the material. This paper presents an experimental method for determining the value of this f_F parameter for one of the basic structural steel types used in construction, S235JR steel. The case of a low initial level of stress triaxiality η implemented by means of tensile specimens without notches is considered. For a smooth unloaded specimen, stress triaxiality reaches its limit, a minimal value. At the beginning of the deformation process, when there are no signs of the necking phenomenon, there is no initial notch (notch radius $\rho_0 = \infty$). Basing on the stress triaxiality defined as $\eta = 1/3 + \ln[(r_0/2\rho_0) + 1]$, where r_0 denotes the initial minimal radius of the specimen's cross-section, for unloaded, smooth tensile specimen without a notch, the initial stress triaxiality is $\eta = 1/3$, and is the lowest possible. Obviously, η may change over time as a result of deformation; these changes are dependent on the initial value of stress triaxiality, but this problem is not analysed in the study. After necking the triaxiality is changed and in some points it may not be low at fracture. The concept of the method applied should be emphasized, as it is quite unique in comparison to the methods widely used, which are all based on the calibration of the parameters. The value of void volume fraction f_F at failure was determined by the application of digital image analysis of fracture surfaces of S235JR steel, taking into consideration real, physical results obtained directly from the material tested.

2. VOID VOLUME FRACTION IN A GTN MATERIAL MODEL

As mentioned above, the original Gurson model was developed over the span of several years. One significant modification was the redefinition by Tvergaard and Needleman of the void volume fraction according to the following function [18]:

$$f^* = \begin{cases} f & \text{for } f \leq f_c \\ f_c + \frac{1/q_1 - f_c}{f_F - f_c} (f - f_c) & \text{for } f_c < f \end{cases} \quad (2)$$

where: f_c – critical void volume fraction corresponding to the onset of void coalescence, f_F – critical void volume fraction corresponding to material failure.

This modified void volume fraction f^* was introduced into the GTN yield potential (1) in order to describe the changes in the stress state taking place during deformation due to void nucleation and growth. According to the Nahshon and Hutchinson modification, the evolution law for the void includes the shear effect. Gurson's original void volume fraction f concept was modified in order to describe the phenomena observed for the range of deformation when the value of f is higher than the critical parameter f_c , corresponding to the onset of void coalescence. As can be seen from eq. (2) in these regards, the modified value of the void volume fraction is dependent on three material parameters, critical void volume fraction f_c , Tvergaard's coefficient q_1 , and critical void volume fraction f_F which corresponds to material failure. The critical f_F parameter defines the void volume fraction observed in the material's microstructure at final failure, when decohesion is observed. Thus, this may be treated as a material constant, a criterion parameter which determines material rupture.

3. PROPERTIES OF THE TESTED MATERIAL

Mild, low-carbon S235JR steel used in civil engineering as a common grade material is evaluated in this study. The chemical composition of the tested material meets the standard requirements [25], the content proportions of the elements are: C = 0.14 %, Mn = 0.54 %, Si = 0.15 %, P = 0.016 %, S = 0.026 %, Cu = 0.28 %, Cr = 0.12 %, Ni = 0.10 %, Mo = 0.02 %, V = 0.002 % and N = 0.01 %. As is typical for this kind of steel, inclusions and second-phase particle are observed in the microstructure; being impurities they make the voids nucleated and growing during the deformation process. The mechanical properties

of the tested S235JR steel shown in Table 1 were determined in a standard tensile test, according to [26].

Table 1. Mechanical properties of the tested S235JR steel

$n = 3$	E [MPa]	$R_{p0.2}$ [MPa]	R_{eH} [MPa]	R_{eH}/R_m [%]	R_{eL} [MPa]	A_e [%]	R_m [MPa]	F_m [kN]	$A_{gt(corr)}$ [%]	A_g [%]	R_b [MPa]	$A_t(corr)$ [%]
\bar{x}	225	353	362	73.93	343	2.89	490	38.48	19.34	19.12	324	27.7
s	8	2	5	0.91	4	0.07	2	0.12	0.18	0.19	6	1.0
v	3.57	0.70	1.50	1.23	1.15	2.28	0.31	0.31	0.95	0.97	1.86	3.77

The stress-strain curves determined during the experiments are presented in Fig. 2. Mechanical properties of S235JR steel are typical, though significantly higher than the standard requirements [25].

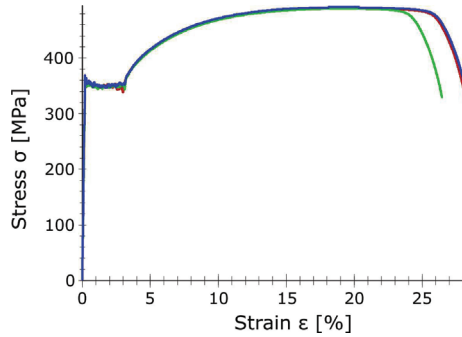


Fig. 2. Nominal stress-strain curves for S235JR steel determined during tensile tests

4. EXPERIMENTAL DETERMINATION OF THE VOID VOLUME FRACTION AT FAILURE FOR S235JR STEEL

In order to determine the void volume fraction at failure for S235JR steel, a two-step procedure was applied. First, the static tensile tests were conducted; these are the same experiments which were described in the previous section. Standard round specimens of a nominal diameter of 10 mm were used, according to the requirements described in [26]. Specimens were tensiled up to total failure in order to obtain fracture surfaces necessary for further research, as shown in Fig. 3.

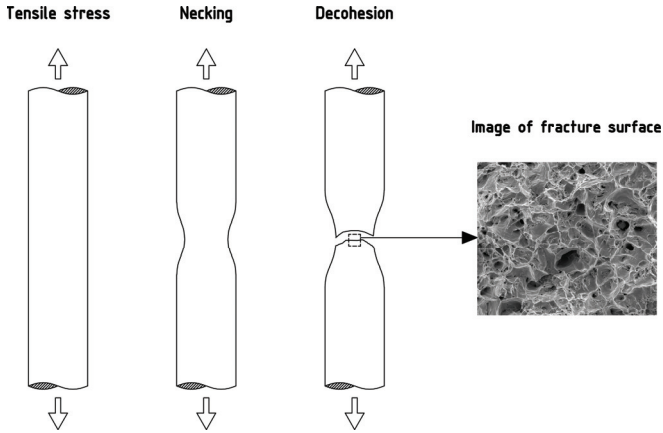


Fig. 3. Scheme of specimen preparation for image analysis of fracture surfaces of S235JR steel

In the next step, the analysis of the fractured surfaces was performed. The main concept of measurement acquisition is directly based on phenomena observed during the failure process taking place in the microstructure of the metals, as presented in the introduction section. Taking into consideration Gurson's basic concept of the damage parameter represented by the void volume fraction in order to determine its critical value f_F , it was necessary to measure its quantity on fractured surfaces. For this purpose, the samples were cut off from separate parts of specimens subjected to static tension (Fig. 3). Then, the fracture surfaces were analysed by scanning microscope technique. Magnifications ranging from $\times 500$ to $\times 5000$ were used in order to test and optimize measurements taken for different settings. A sample photograph of one of the input fracture surfaces is presented in Fig. 4. It may be treated as a representative fracture surface, as differences between particular surfaces for magnifications ranging from $\times 500$ to $\times 5000$ were negligible. For these magnifications, the shapes of the surfaces are similar, which results in slight deviations in measured values of the void volume fraction of f_F .

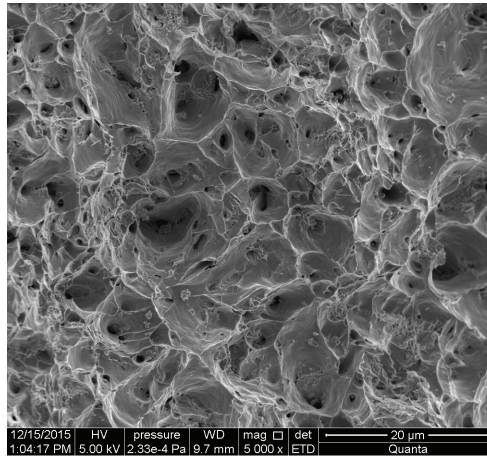


Fig. 4. S235JR fracture surface

The formations of void coalescence which lead to the material's decohesion are clearly visible; they are dark grey. Between these regions, ligaments linking the void formations exist. They are brighter than the voids. These differences in colours of particular areas, i.e. the voids and ligaments, make it possible to differentiate them. For this purpose, the method of quantitative image analysis was applied. As a first step, the input images of a fracture surface (Fig. 5) were converted into two-tone images, based on a colour differential criterion for voids and their ligaments. As an effect, two-colour (binarized) images were obtained, where void and intervoid ligaments were represented by two colours only. Next, the regions representing the voids were removed. The images showing the intervoid ligaments were obtained, as shown on an exemplary image in Fig. 5.

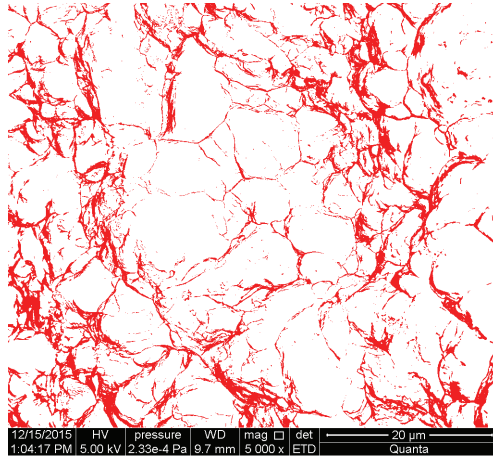


Fig. 5. Two-colour (binarized) image of an S235JR fracture surface

The dimensions of the voids observed on the photographs of the fracture surfaces ranging from $2\ \mu\text{m}$ up to $10\ \mu\text{m}$ are predominant. Sporadically, single voids appear larger. The shape of the void at the failure moment is similar to a circle. Thus, it can be established that the predominant area of voids is ranging from $3.14\ \mu\text{m}^2$ up to $78.5\ \mu\text{m}^2$.

At this final stage it was possible to measure the areas of the voids. An automatic graphical method was applied by scanning the areas in white, representing the voids. The measured area was then divided by the total surface area of the entire image in order to calculate a relative surface representing the void volume fraction. For images taken from fractured specimens this represents the void volume fraction at the final failure of material.

5. RESULTS AND DISCUSSION

Basing on the digital image analysis of fracture surfaces of S235JR steel described in the previous section, void volume fraction f_V was obtained. The voids were identified on binarized images of fracture surfaces of S235JR specimens used in the tensile tests, as shown in the two-colour (binarized) image of the S235JR fracture surface visible on Fig. 5, where white colour represents the voids. The values of f_V

were identified as relative areas of voids on fracture surfaces of S235JR. The relative area of voids was calculated as the ratio of the area of voids - the white area shown in the exemplary Fig. 5 - to the whole area of the fracture surface. The procedure described above was repeated for 34 images taken from S235JR steel samples. In order to obtain statistically significant results, Chauvenet's criterion was used. Atypical results were rejected from total data, and the final analysis was performed for the 30 samples which met Chauvenet's statistical criterion. The measured values of f_F for the images ranged from 0.648 up to 0.807, while standard deviation was 0.045. A value of $f_F = 0.741$ was obtained as a mean value of void volume fractions measured for the 30 samples.

As a result of the performed analysis, the critical value of void volume fraction f_F at the final failure of S235JR steel was determined. For the considered case of low initial stress triaxiality $\eta = 1/3$, a value of $f_F = 0.741$ was determined. This value may be used to describe the plasticity behaviour of S235JR steel taking into consideration the effect of microdefects by using the Gurson-Tveergard-Needleman model, when low initial stress triaxialities are observed.

The obtained value $f_F = 0.741$ is slightly higher than the typical value used for many metals, $f_F = 0.667$. The difference is about 10 %, so it can be concluded that volume fraction f_F at the moment of failure determined experimentally based on the fracture surfaces of the material is in the same range as the theoretical values derived from the GTN material model.

On the other hand, taking into account the results obtained by authors who often use calibration methods, the value determined experimentally is significantly higher. The range of critical values of the void volume fraction at failure for a wide range of metals is suggested as $f_F = 0.15 \div 0.25$, according to [18, 27].

However, the highest values of f_F are also reported, especially for materials with high porosity, as, for example, nodular cast iron, for which the critical value of the void volume fraction at failure is assumed as $f_F = 0.4$ [28]. This is an intermediate value between the value determined in this study $f_F = 0.740877$ and values $f_F = 0.15 \div 0.25$ calibrated for many metals.

It should be clearly emphasized that the critical void volume fraction at failure determined based on the presented experimental methods is a value measured taking into consideration the area of voids related to the area of the entire fractured surface. Having regarded the inhomogeneity of the voids' shape and their anisotropy, the precise determination of their relative volume is very complex and sensitive based on image analysis.

The second remark concerns the changes in stress triaxiality observed during the deformation process of the material, which may slightly vary. Thus, it is strongly highlighted that the scope of analysis as well

as the results obtained are valid for S235JR steel at a stage of low initial stress triaxiality, observed for smooth elements without notches and cracks at the beginning of the deformation.

In order to validate the results obtained, a simulation of a steel specimen subjected to tension using the GTN material model with an experimentally determined parameter f_F has been performed.

In the following numerical simulation, a tensile element made from the basic steel grade used in construction, S235JR, was analyzed. Calculations were made via Abaqus 6.10 using explicit nonlinear dynamic analysis. A model of a smooth tensile bar of a circular cross-section was built. It was modeled as axially symmetric using standard CAX4R elements. Due to the symmetry of the problem, $\frac{1}{4}$ of the sample was modeled. In the area near the crack plane a mesh of dimensions corresponding to the so-called characteristic length determined for S235JR steel as $250\ \mu\text{m}$ was applied (Fig. 6).

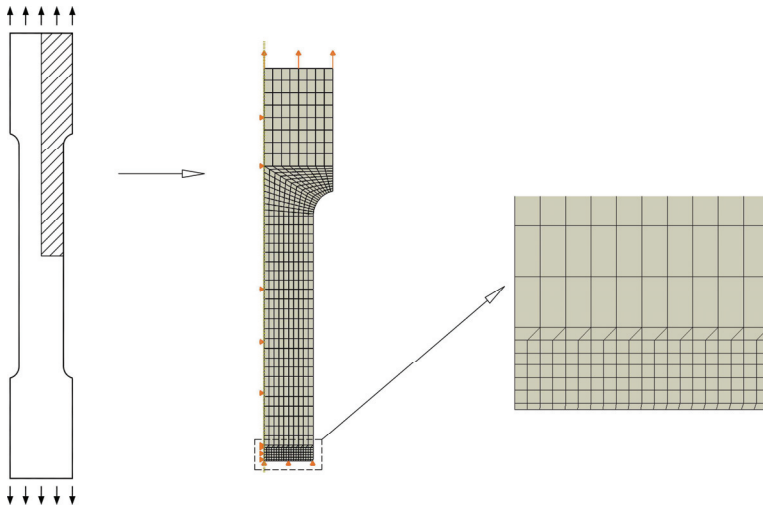


Fig. 6. Numerical model of the analyzed tensiled specimen

During analysis, the modified GTN material model was used assuming the values of the material parameters for S235JR steel given in Table 2.

Table 2. GTN material model parameters for S235JR steel

Initial void volume fraction f_0	Critical void volume fraction f_c	Critical void volume fraction at failure f_F	Tvergaard's parameters			Mean strain for void nucleation ε_N	Volume fraction of void nucleating particles f_N	Standard deviation of nucleation strain s_N
			q_1	q_2	q_3			
0.001	0.06	0.200 0.741	1.91	0.79	3.65	0.30	0.04	0.05

As it can be seen, two values of critical void volume fraction at failure f_F were considered in order to compare and validate the results obtained; $f_F = 0.2$, corresponding to the mean value calibrated for many metals, and $f_F = 0.741$, determined experimentally.

Figure 7 shows the force-elongation curves $F(l)$ obtained during the experiments and numerical simulations.

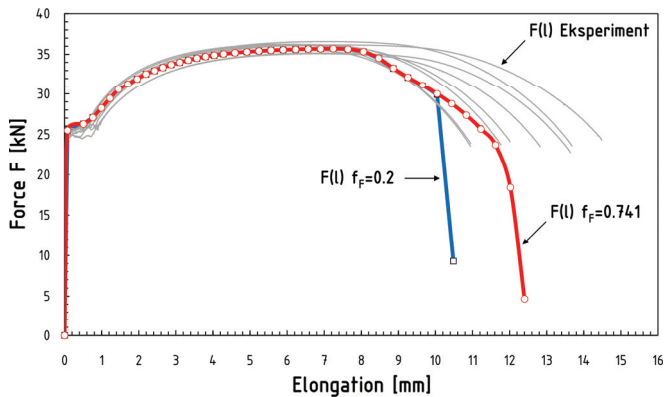


Fig. 7. The force-elongation curves $F(l)$ obtained during the experiments and numerical simulations.

As it can be seen, by assuming the critical value $f_F = 0.20$, which corresponds to the volume of microdamages observed at the time of failure for many metal materials, results show earlier damage than at the value of $f_F = 0.741$ determined experimentally. Thus, the force-elongation curves $F(l)$ determined

numerically by using the GTN material model and a value of $f_F = 0.741$ are closer to the experimental results when compared to the assumed value $f_F = 0.20$. It can be concluded that the experimentally determined value of $f_F = 0.741$ enables accurate modelling of the decohesion processes observed in S235JR steel and prediction of its failure.

6. CONCLUSIONS

As can be seen from the results obtained, application of an experimental method is made possible for determining and analyzing one of Gurson-Tvergaard-Needleman damage model's parameters for structural steel. In comparison to the much used method based on a curve-fitting procedure, where material parameters are calibrated in order to achieve agreement between experimental and model results, it was possible to determine material parameters taking into consideration real, physical results. By applying the quantitative image procedure the value of the void volume fraction at failure for S235JR steel in the case of low initial stress triaxiality was obtained. This result may be useful for modelling the behaviour of S235JR steel based on the GTN damage material model.

REFERENCES

1. L. M. Kachanov, "Time of the rupture process under creep conditions", *Izvestiya Akademii Nauk SSSR, Otdelenie Tekhnicheskikh Nauk*: 8, 26–31, 1958.
2. A. L. Gurson, "Continuum theory of ductile rupture by void nucleation and growth: Part I – Yield criteria and flow rules for porous ductile media", *Journal of Engineering Materials and Technology (ASME)*: 99, 2–15, 1977.
3. V. Tvergaard, "Influence of voids on shear band instabilities under plane strain conditions", *International Journal of Fracture*: 17, 389 – 407, 1981.
4. P. Suquet, "Plasticité et homogénéisation", *Dissertation: Thèse d'Etat: Sciences Mathématiques (Mécanique théorique)*: Paris 6, Université Pierre et Marie Curie, Paris, 1982.
5. J. P. Cordebois, F. Sidoroff, "Endommanegement Anisotrope En Élasticité et Plasticité", *Journal de Mécanique Théorique et Appliquée, Numéro Spécial*, 45 – 60, 1982.
6. J. Lemaitre, "How to use damage mechanics", *Nuclear Engineering and Design*: 80, 233–245, 1984.
7. J. Lemaitre, "A continuous damage mechanics model for ductile fracture", *Journal of Engineering Materials and Technology*: 107, 83 – 89, 1985.
8. A. Dragon, A. Chihab, "Quantifying of ductile fracture damage evolution by homogenization approach", *Transactions of the 8th International Conference on Structural Mechanics in Reactor Technology, Centre de Conférences Albert Borschette, Brussels, Belgium, Aug. 19–23, 1985, v. L. Inelastic behaviour of materials and constitutive equations*, 305– 310, 1985.
9. G. Rousselier, "Ductile fracture models and their potential in local approach of fracture", *Nuclear Engineering and Design*: 105, 97–111, 1987.
10. J. Murzewski, "Brittle and ductile damage of stochastically homogeneous solids", *International Journal of Damage Mechanics*: 1, 276– 289, 1992.

11. G. Z. Voyiadjis, P. I. Kattan, "A plasticity-damage theory for large deformation of solids – Part I: Theoretical formulation" *International Journal of Engineering Science*: 30, 1089–1108, 1992.
12. C. L. Chow, T. J. Lu, "An analytical and experimental study of mixed-mode ductile fracture under nonproportional loading" *International Journal of Damage Mechanics*: 1, 191–236, 1992.
13. K. Saanouni, C. H. Foster, F. B. Hatira, "On the anelastic flow with damage", *Int. J. Damage Mech.*: 3, 140–169, 1994.
14. S. F. Taher, M. H. Baluch, A. H. Al-Gadhib, "Towards a canonical elastoplastic damage model", *Engineering Fracture Mechanics*: 48, 151–166, 1994.
15. P. G. Kossakowski, "The influence of microstructural defects on the stress state of S235JR steel under plastic deformation", *Solid State Phenomena*: 250, 69–76, 2016.
16. P. G. Kossakowski, "Microstructural failure criteria for S235JR steel subjected to spatial stress states", *Archives of Civil and Mechanical Engineering* 15: 195–205, 2015.
17. V. Tvergaard, Influence of voids on shear band instabilities under plane strain conditions, *International Journal of Fracture*: 17, 389–407, 1981.
18. V. Tvergaard, A. Needleman, "Analysis of the cup-cone fracture in a round tensile bar", *Acta Metallurgica*: 32, 157–169, 1984.
19. K. Nahshon, J.W. Hutchinson, "Modification of the Gurson Model for shear failure", *European Journal of Mechanics A/Solids*: 27, 1–17, 2008.
20. P. G. Kossakowski, "Stress Modified Critical Strain criterion for S235JR steel at low initial stress triaxiality", *Journal of Theoretical and Applied Mechanics*: 52, 995–1006, 2014.
21. P. G. Kossakowski, W. Wcislik, "Experimental determination and application of critical void volume fraction f_c for S235JR steel subjected to multi-axial stress state", in: T. Lodygowski, J. Rakowski, P. Litewka (Eds.), *Recent Advances in Computational Mechanics*, CRC Press/Balkema, London, 303–309, 2014.
22. W. Wcislik, "Numerical determination of critical void nucleation strain in the Gurson-Tvergaard-Needleman porous material model for low stress state triaxiality ratio", *Proceeding of METAL 2014: 23rd International Conference on Metallurgy and Materials*, Brno, 794–800, 2014.
23. P. G. Kossakowski, W. Wcislik, "Effect of critical void volume fraction f_f on results of ductile fracture simulation for S235JR steel under multi-axial stress states", *Key Engineering Materials – Fracture and Fatigue of Materials and Structures* 598: 113–118, 2014.
24. P. G. Kossakowski, "An analysis of the Tvergaard parameters at low initial stress triaxiality for S235JR steel", *Polish Maritime Research*: 21, 100–107, 2014
25. PN-EN 10025-2:2007 Hot-rolled structural steel. Part 2 – Technical delivery conditions for non-alloy structural steels.
26. PN-EN 10002-1:2004 Metallic materials – Tensile testing – Part 1: Method of test at ambient temperature.
27. Z. L. Zhang, C. Thaulow, J. Ødegård, "A Complete Gurson model approach for ductile fracture", *Engineering Fracture Mechanics*: 67, 155–168, 2000.
28. K. Taghizadeh, "Implementation of a shear-modified Gurson-Model into the FE-Program Abaqus", Master Thesis, Technische Universität Bergakademie Freiberg, 2014.

LIST OF FIGURES AND TABLES:

Fig. 1. Mechanism of ductile fracture (based on [15, 16])

Rys. 1. Mechanizm pęknięcia ciągliwego (w oparciu o [15, 16])

Fig. 2. Nominal stress-strain curves for S235JR steel determined during tensile tests

Rys. 2. Nominalne krzywe napężenie-odkształcenie wyznaczone w próbie rozciągania stali S235JR

Fig. 3. Scheme of specimen preparation for image analysis of fracture surfaces of S235JR steel

Rys. 3. Schemat przygotowania próbek do analizy obrazowej powierzchni pęknięć stali S235JR

Fig. 4. S235JR fracture surface

Rys. 4. Powierzchnia pęknięcia stali S235JR

Fig. 5. Two-colour (binarized) image of S235JR fracture surface

Rys. 5. Dwukolorowy (binaryzowany) obraz powierzchni zniszczenia stali S235JR

Fig. 6. Numerical model of analyzed tensiled specimen

Rys. 6. Model numeryczny analizowanej próbki rozciąganej

Fig. 6. The force-elongation curves $F(l)$ obtained during experiments and numerical simulations

Rys. 6. Krzywe siła-wydłużenie $F(l)$ uzyskane podczas eksperymentów i symulacji numerycznych

Tab. 1. Mechanical properties of tested S235JR steel

Tab. 1. Właściwości mechaniczne badanej stali S235JR

Tab. 2. GTN material model parameters for S235JR steel

Tab. 2. Parametry materiałowe modelu GTN stali S235JR

Received 28.11.2016

Revised 19.03.2018

ANALIZA KRYTYCZNEGO UDZIAŁU OBJĘTOŚCIOWEGO PUSTEK W MOMENCIE ZNISZCZENIA STALI S235JR PRZY NISKIM WSTĘPNYM STOPNIU TRÓJOSIOWOŚCI NAPRĘŻEŃ

Słowa kluczowe: udział objętościowy pustek, zniszczenie, stal S235JR, model materiałowy Gursona-Tvergaarda-Needlemana, niski stopień trójosiowości naprężeń.

STRESZCZENIE:

Tematem pracy są zagadnienia związane z mechanizmami towarzyszącymi procesowi niszczenia stali konstrukcyjnej S235JR. Zakres badań obejmował końcową fazę uplastycznienia materiału, aż do momentu jego zniszczenia. W przeprowadzonej analizie oparto się na podejściu mechaniki zniszczenia, wykorzystując model materiału porowatego Gursona-Tvergaarda-Needlemana (GTN). Zbadano jeden z podstawowych parametrów mikrostruktury GTN, krytyczny udział objętościowy pustek f_F . Współczynnik ten determinuje proces niszczenia materiału od chwili wzrostu i łączenia się mikrodefektów struktury materiałowej, aż do dekohezji materiału w skali makro. Badania przeprowadzono dla przypadku niskiego wstępnego stopnia trójosiowości naprężeń $\eta = 1/3$. W odróżnieniu od najpopularniejszych metod, takich jak np. procedura dopasowania parametrów analizy do krzywych wzorcowych, zaproponowano metodę eksperymentalną, opartą na analizie rzeczywistych obrazów powierzchni pęknięć stali S235JR uzyskanych doświadczalnie. Cyfrowa analiza obrazowa powierzchni pęknięć pozwoliła na określenie wartości udziału objętościowego pustek f_F w momencie zniszczenia materiału, co umożliwiło eksperymentalne wyznaczenie krytycznego parametru f_F dla stali S235JR. W pracy przedstawiono również wyniki analizy numerycznej, weryfikującej rezultaty uzyskane w badaniach doświadczalnych. Symulowano przypadek rozciągania statycznego elementu o przekroju kołowym, który modelowano przy zastosowaniu modelu materiału GTN. Wyznaczone wartości parametru f_F pozwoliły na symulację procesu uplastycznienia stali S235JR oraz przewidzenie momentu jej zniszczenia.